Electronic Supplementary Information (ESI)

Engineering on the edge of Pd nanosheet cocatalysts for enhanced photocatalytic reduction of CO_2 to fuels

Yuzhen Zhu,[a] Zaixiang Xu,[a] Wenya Jiang,[b] Shuxian Zhong,[a] Leihong Zhao[a] and Song Bai*[a,b]

[a] Key Laboratory of the Ministry of Education for Advanced Catalysis Materials, College of Chemistry and Life sciences, Zhejiang Normal University, Jinhua, Zhejiang, 321004, P. R. China.
[b] School of Chemistry and Materials Science, University of Science and Technology of China, Hefei, Anhui, 230026, P. R. China.

E-mail: songbai@zjnu.edu.cn

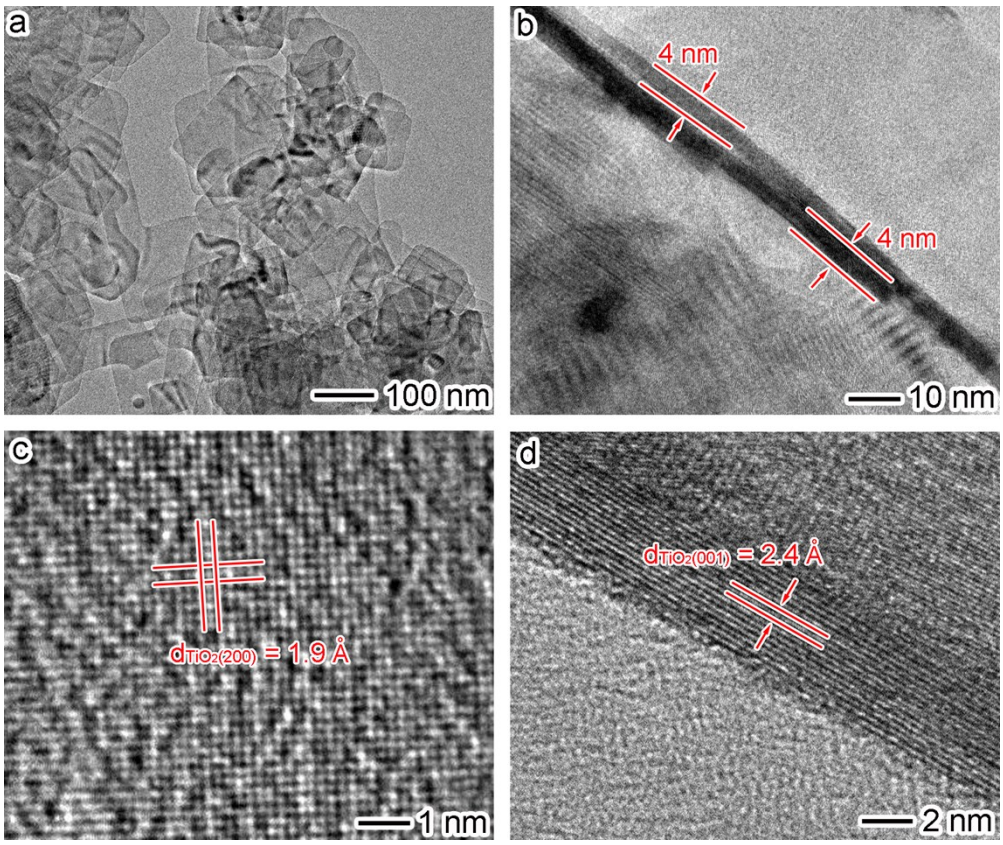

Fig. S1 TEM and HRTEM images of TiO_2 nanosheets: (a) TEM image showing the flat surface of nanosheets; (b) TEM image showing the cross section and thickness of the nanosheets; (c) HRTEM image showing the lattice fringes of the flat faces; (d) HRTEM image showing the lattice fringes of side faces.

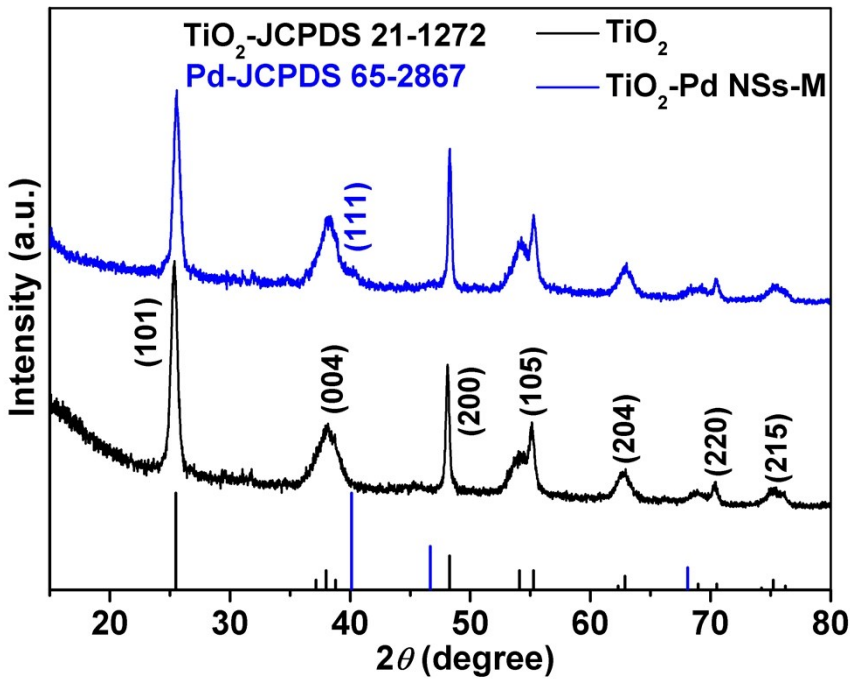

Fig. S2 XRD patterns of TiO_2-Pd NSs-M in reference to bare TiO_2 nanosheets. The standard diffraction patterns for anatase TiO_2 (JCPDS 21-1272) and *fcc* Pd (JCPDS 65-2867) are provided as references.

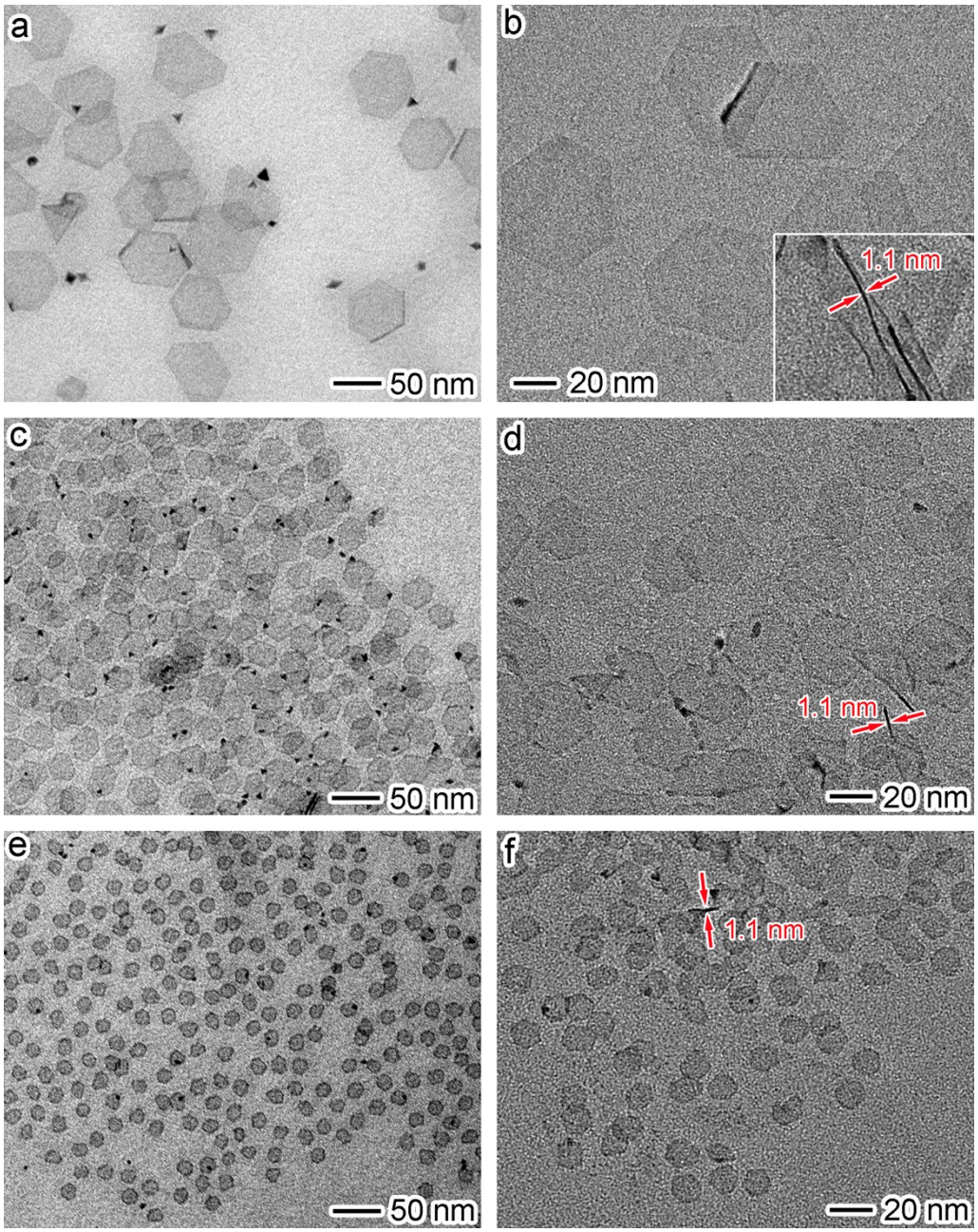

Fig. S3 TEM images of (a,b) large, (c,d) middle and (e,f) small Pd nanosheets.

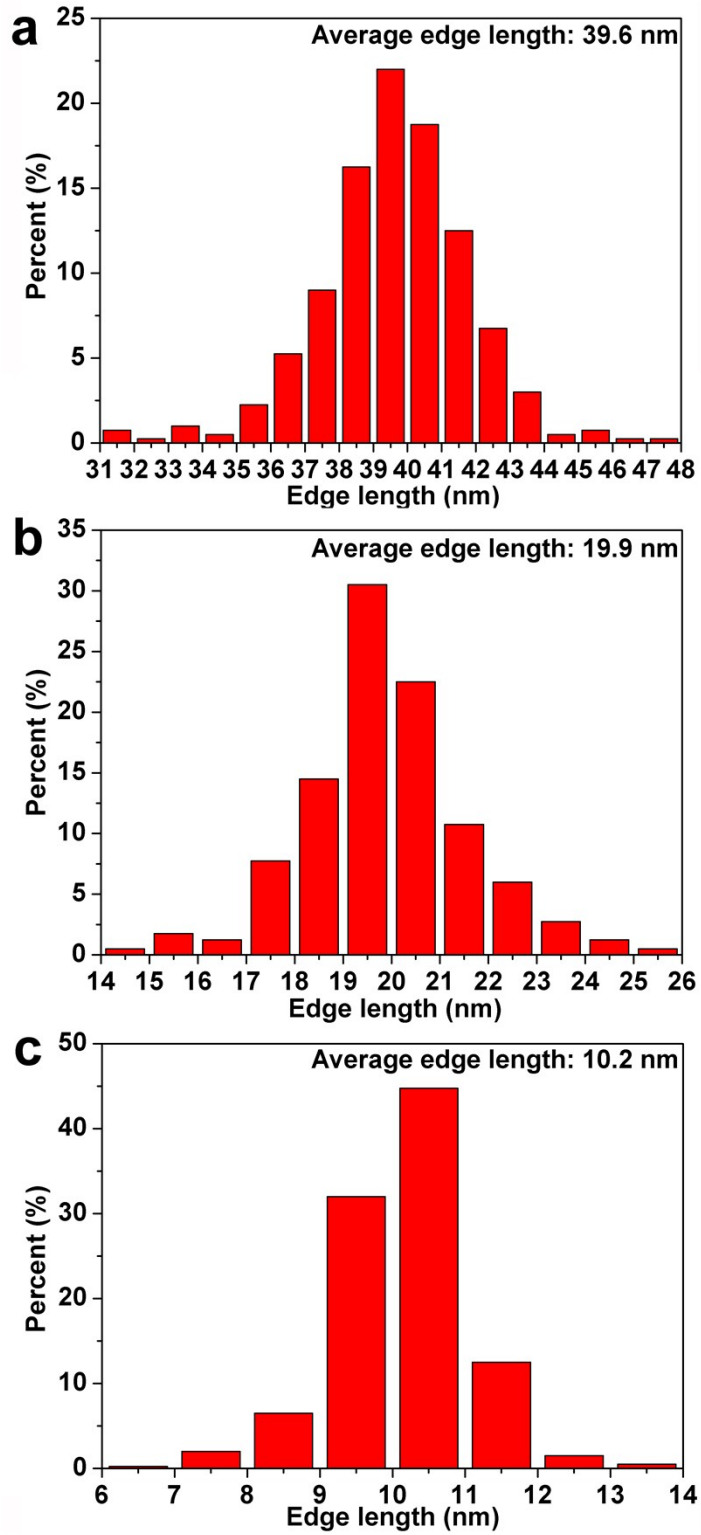

Fig. S4 Edge length distribution histograms of the as-prepared Pd nanosheets on the TiO_2 nanosheets: (a) TiO_2-Pd NSs-L, (b) TiO_2-Pd NSs-M, (c) TiO_2-Pd NSs-S.

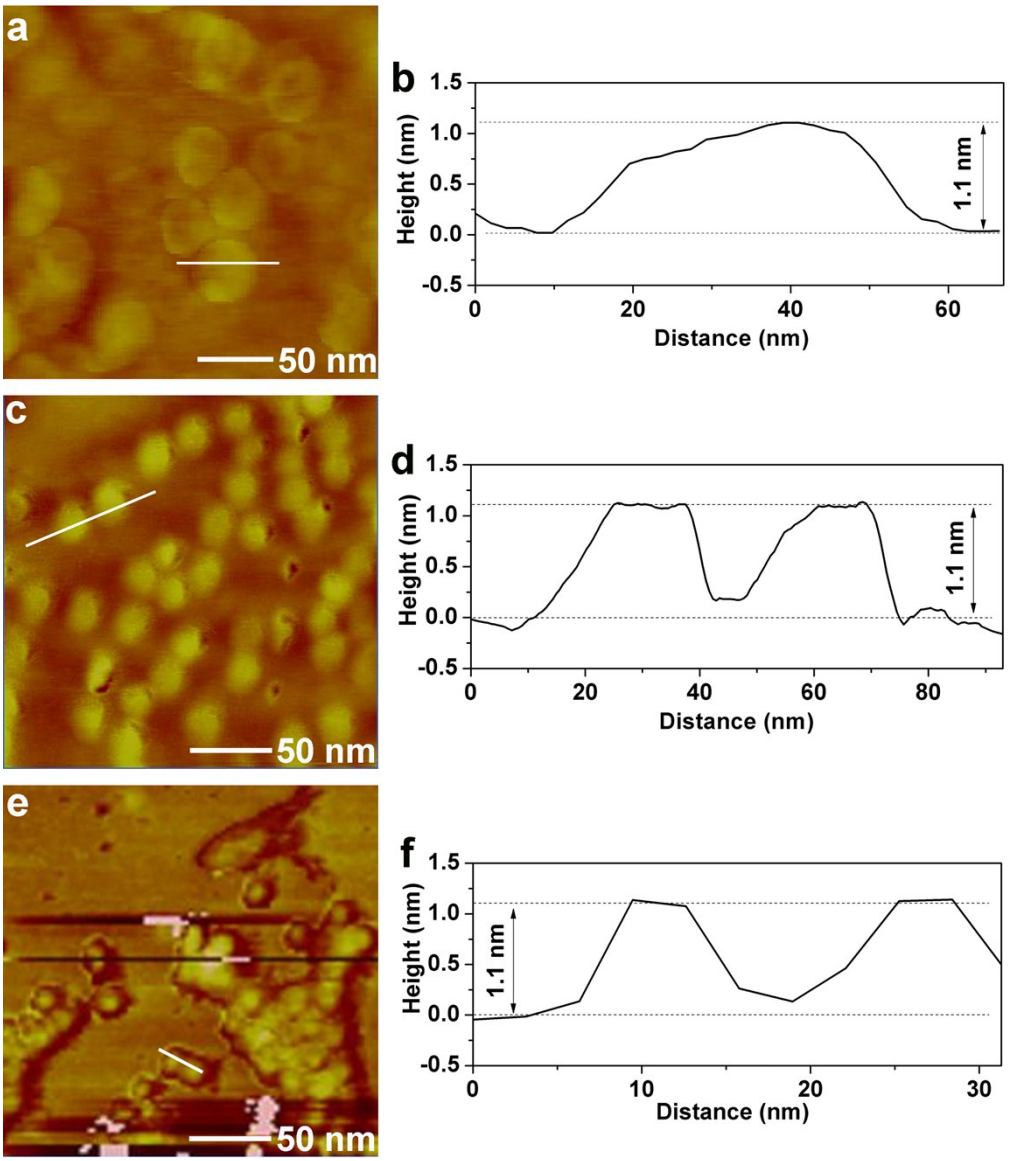

Fig. S5 AFM images and the corresponding height profiles of Pd nanosheets in (a,b) large, (c,d) middle and (e,f) small size.

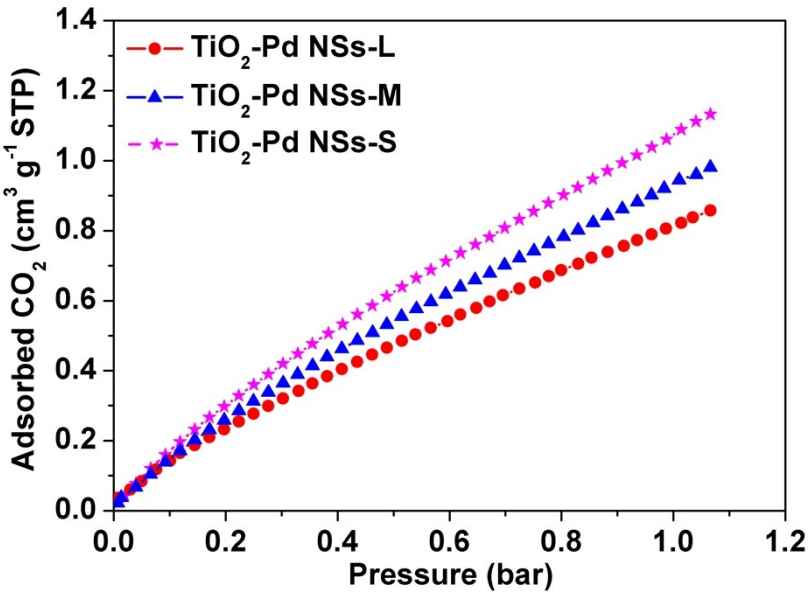

Fig. S6 CO_2 adsorption behaviors for TiO_2-Pd NSs samples. The data are plotted based on the total weights of materials.

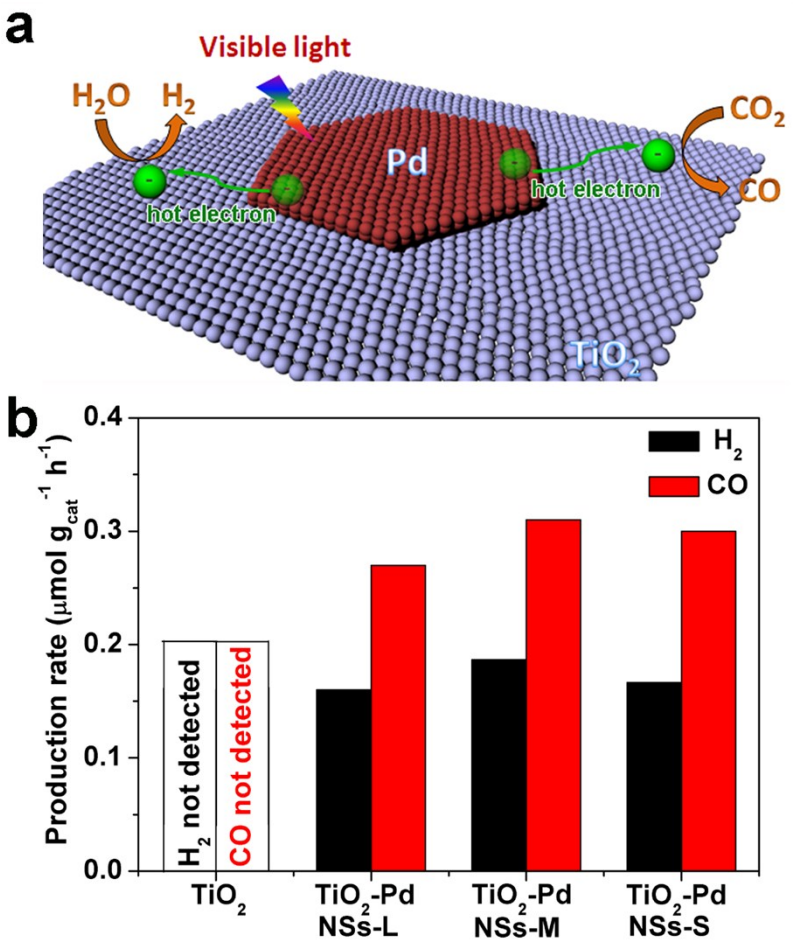

Fig. S7 (a) Schematic illustration of the photocatalytic mechanism of TiO_2-Pd NSs samples under visible light irradiation; (b) H_2 and CO average evolution rates of TiO_2-Pd NSs samples in photocatalytic CO_2 reduction reaction with bare TiO_2 as a reference sample under visible light irradiation (400 nm $<$ λ $<$ 780 nm).

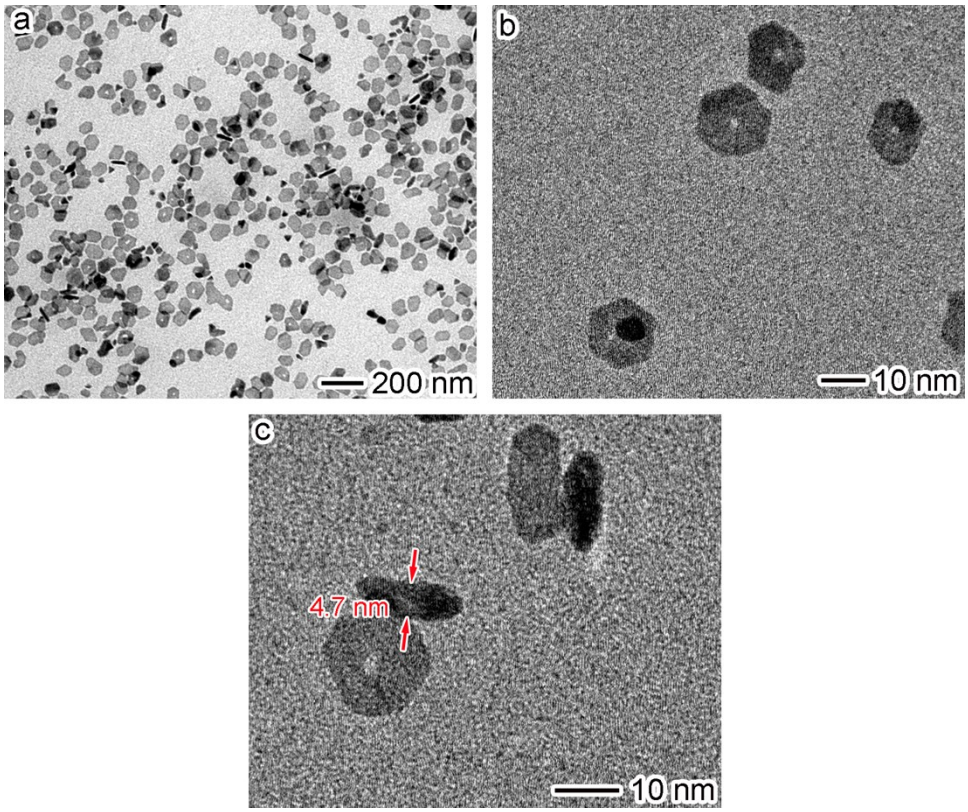

Fig. S8 TEM images of small Pd nanorings.

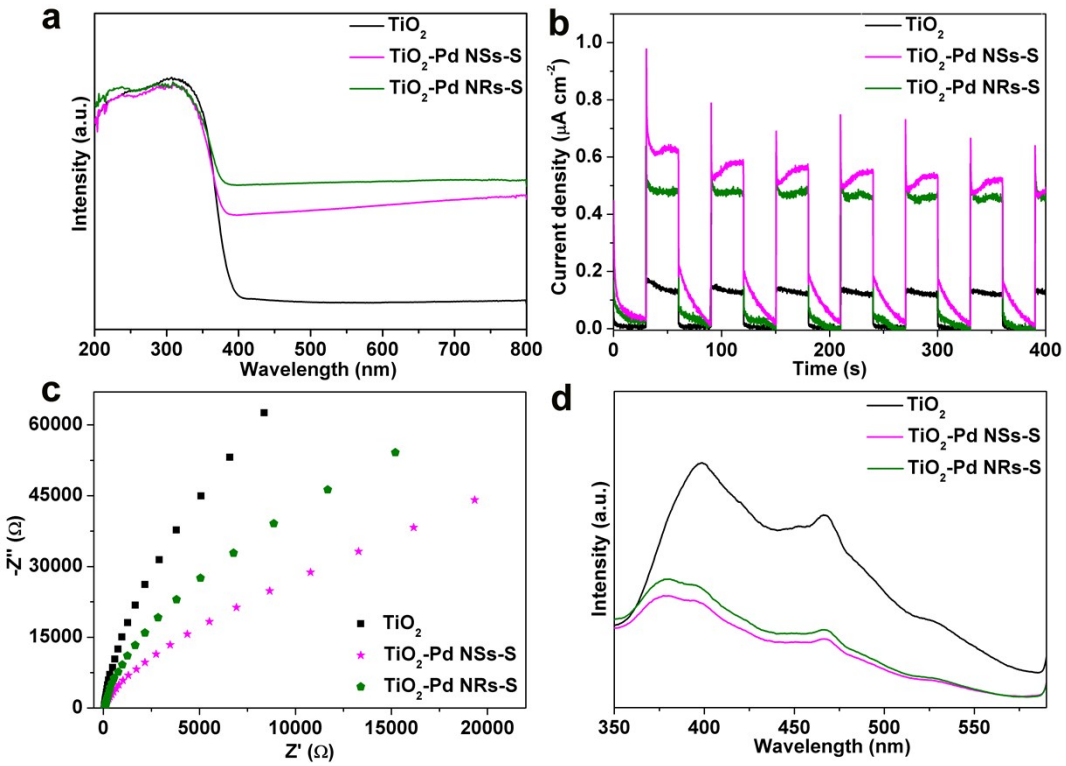

Fig. S9 (a) UV-vis-NIR diffuse reflectance spectra of bare TiO_2, TiO_2-Pd NSs-S and TiO_2-Pd NRs-S; (b) photocurrent *vs.* time (*I-t*) curves and (c) EIS Nyquist plots of bare TiO_2, TiO_2-Pd NSs-S and TiO_2-Pd NRs-S at 0.4 V *vs.* Ag/AgCl under UV light (λ ＜ 400 nm) irradiation; (d) PL spectra of bare TiO_2, TiO_2-Pd NSs-S and TiO_2-Pd NRs-S excited at 310 nm.

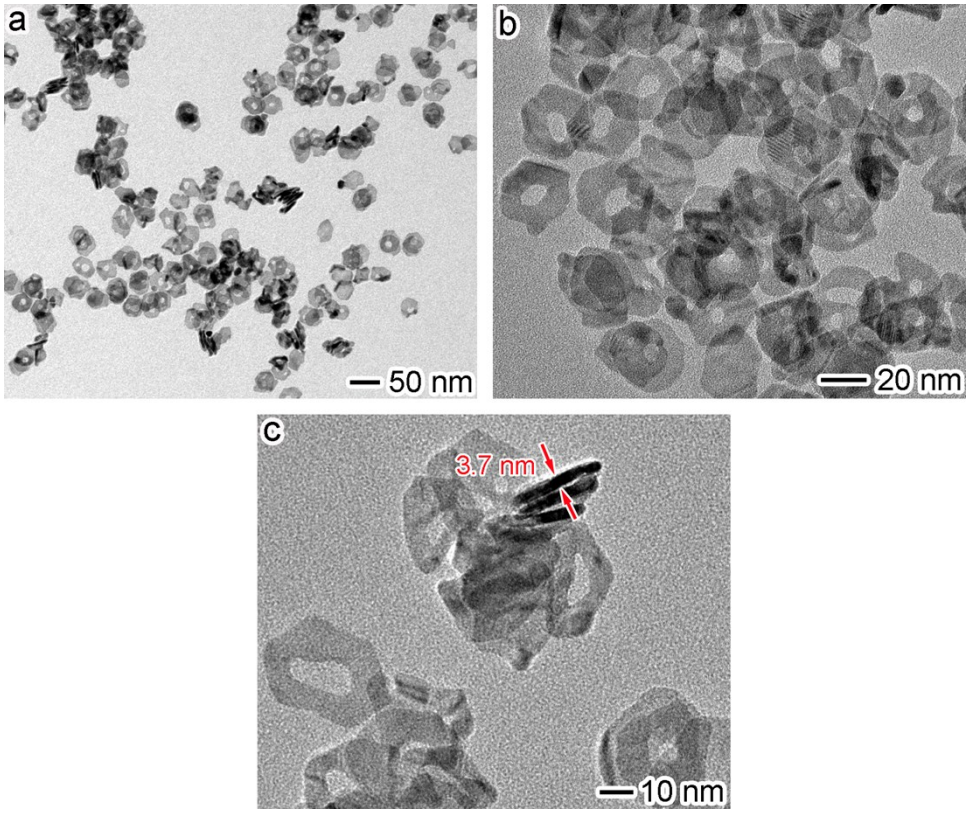

Fig. S10 TEM images of middle Pd nanorings.

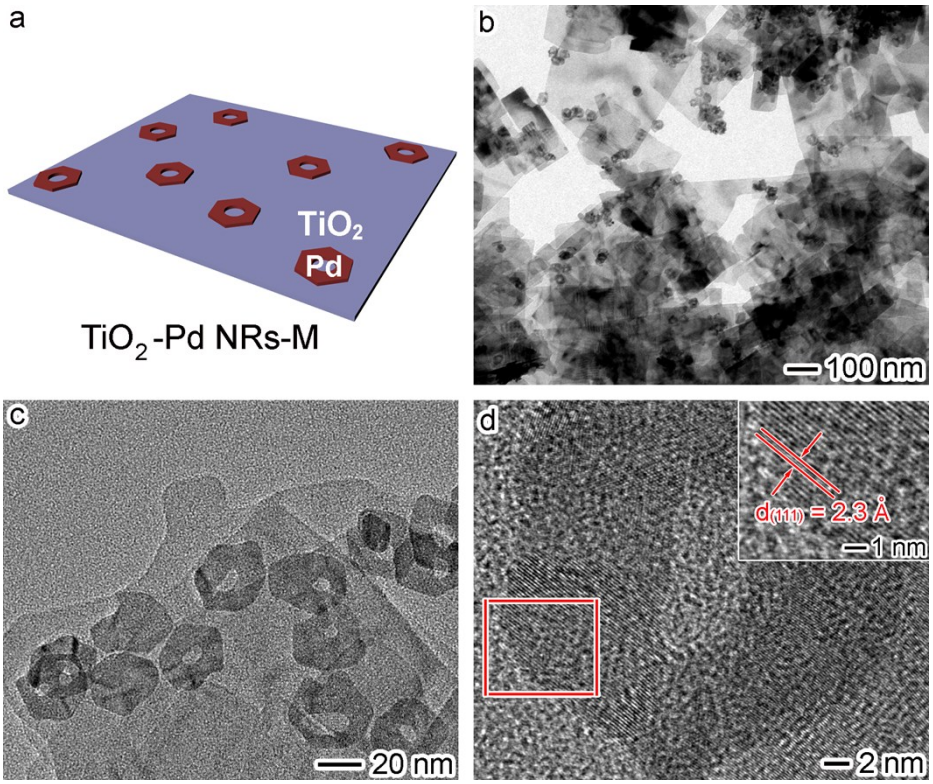

Fig. S11 (a) Schematic illustration, (b,c) TEM and (d) HRTEM images of TiO_2-Pd NRs-M.

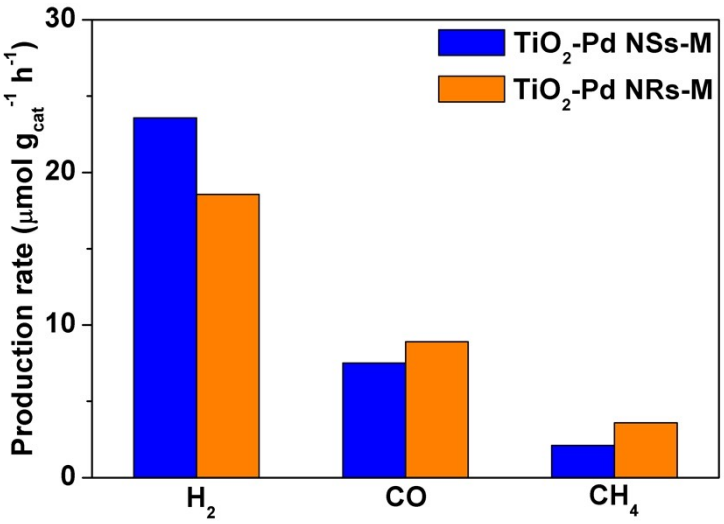

Fig. S12 H_2, CO, and CH_4 average evolution rates of TiO_2-Pd NRs-M in photocatalytic CO_2 reduction reaction with TiO_2-Pd NSs-M as a reference sample.

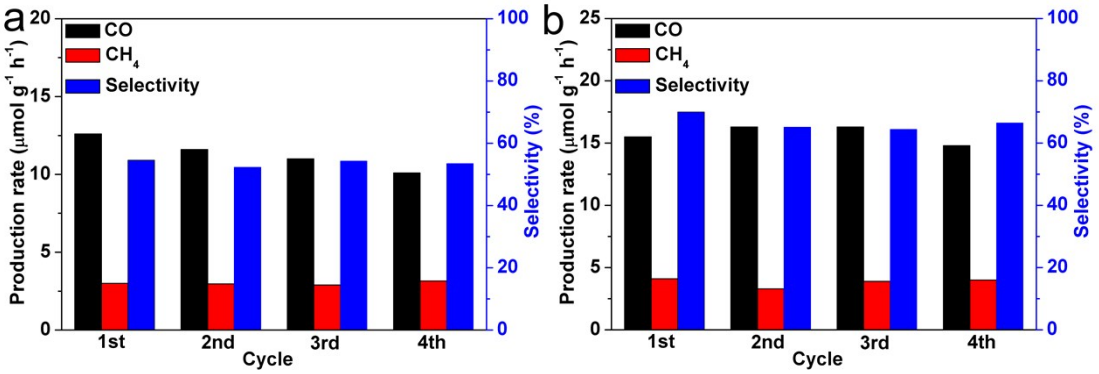

Fig. S13 Stability studies of CO and CH_4 evolution rates as well as the selectivity for CO_2 reduction with (a) TiO_2-Pd NSs-S and (b) TiO_2-Pd NRs-S as catalysts in the photocatalytic cyclic process.

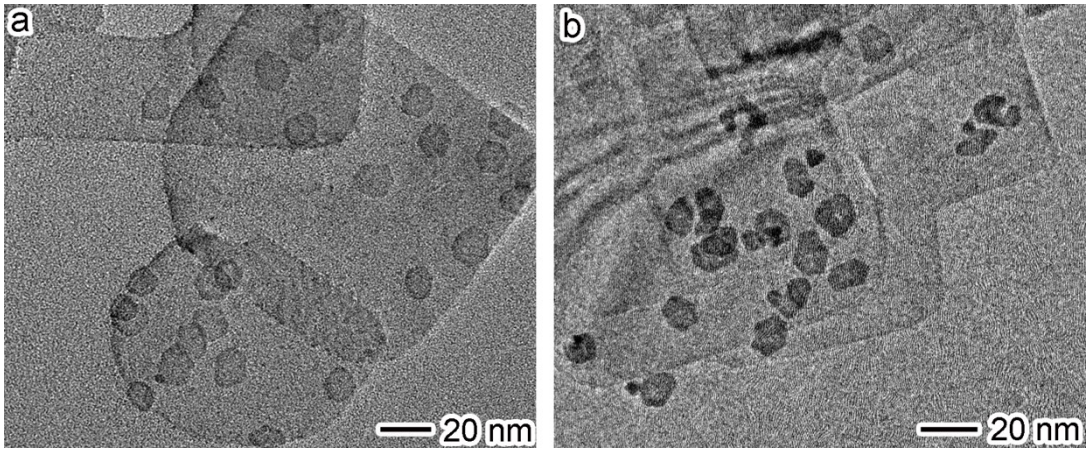

Fig. S14. TEM images of (a) TiO_2-Pd NSs-S and (b) TiO_2-Pd NR-S after the photocatalytic cyclic process.

Table S1. Chemical compositions of the TiO_2-Pd NSs and TiO_2-Pd NRs samples determined by ICP-MS.

Sample	Weight ratio of Pd : TiO_2
TiO_2-Pd NSs-L	4.6%
TiO_2-Pd NSs-M	5.0%
TiO_2-Pd NSs-S	4.8%
TiO_2-Pd NRs-S	4.9%
TiO_2-Pd NRs-M	4.8%